

# SCIENTIFIC REPORTS



OPEN

## Effects of ultraviolet treatment and alendronate immersion on osteoblast-like cells and human gingival fibroblasts cultured on titanium surfaces

Changjoo Jeon<sup>1</sup>, Kyung Chul Oh<sup>1</sup>, Kyu-Hyung Park<sup>2</sup> & Hong Seok Moon<sup>1</sup>

In this study, we evaluated the effects of ultraviolet (UV) treatment and alendronate (ALN) immersion on the proliferation and differentiation of MG-63 osteoblast-like cells and human gingival fibroblasts (HGFs) cultured on titanium surfaces. MG-63 cells were used for sandblasted, large grit, and acid-etched (SLA) titanium surfaces, and HGFs were used for machined (MA) titanium surfaces. SLA and MA specimens were subdivided into four groups ( $n = 12$ ) according to the combination of surface treatments (UV treatment and/or ALN immersion) applied. After culturing MG-63 cells and HGFs on titanium discs, cellular morphology, proliferation, and differentiation were evaluated. The results revealed that UV treatment of titanium surfaces did not alter the proliferation of MG-63 cells; however, HGF differentiation and adhesion were increased in response to UV treatment. In contrast, ALN immersion of titanium discs reduced MG-63 cell proliferation and changed HGFs into a more atrophic form. Simultaneous application of UV treatment and ALN immersion induced greater differentiation of MG-63 cells. Within the limitations of this cellular level study, simultaneous application of UV treatment and ALN immersion of titanium surfaces was shown to improve the osseointegration of titanium implants; in addition, UV treatment may be used to enhance mucosal sealing of titanium abutments.

The placement of dental implants has become an essential method for the treatment of edentulous or partially edentulous patients. Titanium remains the material of choice for dental implants because of its superior biocompatibility and mechanical strength<sup>1</sup>. It spontaneously forms a dense titanium dioxide (TiO<sub>2</sub>) layer at its surface when exposed to air or aqueous electrolytes, which acts as a strong barrier against corrosion and ion release from the metal surface, contributing to high biocompatibility<sup>2,3</sup>. Moreover, this oxide layer enhances protein adsorption after implantation and consequently affects osseointegration, which is defined as “the direct structural and functional connection between ordered, living bone, and the surface of a load-carrying implant”<sup>4-6</sup>.

Dental implants consist of an implant fixture, an implant abutment, and an upper prosthesis. In general, implant fixtures have rough surfaces for enhanced osseointegration, whereas implant abutments are composed of smooth or machined surfaces for prevention of biofilm formation<sup>7</sup>. However, for tissue-level implants, the implant fixtures partly consist of machined surfaces on the coronal portion, while the other portion consists of rough surfaces; hence, two types of surface characteristics co-exist in these implants.

Numerous reports have shown that modifications to the microgeometry and roughness of implant surfaces contribute to the achievement of better osseointegration<sup>8</sup>. Examples of these modifications include subtractive methods, such as blasting, etching, and oxidation, and additive methods such as titanium plasma spraying<sup>9</sup>. However, a drawback resulting from the inherent properties of the titanium material itself still remains: the bioactivity of titanium substantially decreases over time when exposed to air due to the appearance of hydrocarbons, resulting in loss of hydrophilicity<sup>10</sup>. This contamination of titanium surfaces has been shown to be

<sup>1</sup>Department of Prosthodontics, College of Dentistry, Yonsei University, Seoul, 03722, Korea. <sup>2</sup>Department of Prosthodontics, Oral Science Research Center, BK21 Plus Project, College of Dentistry, Yonsei University, Seoul, 03722, Korea. Changjoo Jeon and Kyung Chul Oh contributed equally. Correspondence and requests for materials should be addressed to H.S.M. (email: [hsm5@yuhs.ac](mailto:hsm5@yuhs.ac))

related to the initial affinity for human osteoblasts, causing reduced migration and attachment<sup>11</sup>. A common strategy used to convert the hydrophobic titanium surface to the hydrophilic state was the use of ultraviolet (UV) irradiation, whose effects in this context were reported in the late 1990s<sup>12</sup>. UV-treated titanium surfaces not only exhibited alteration of physiochemical properties, but also showed improvement of biologic capabilities, such as increased cell proliferation and enhanced osteoblast differentiation; this phenomenon was termed as photofunctionalisation<sup>13</sup>.

Bisphosphate application is another method used to increase osteoblastic activity. In contrast to UV treatment which indirectly affects osteoblast functions, bisphosphates affect osteoblastic activity in a more direct manner. Although bisphosphonates have been generally used as antiresorptive agents for bone-related disorders by inhibiting osteoclastic activity<sup>14</sup>, several recent studies have reported that these compounds may increase osteoblastic activity<sup>15–18</sup>. Alendronate (ALN), a type of nitrogen-containing bisphosphonates that is currently one of the most effective agents for treating various bone diseases, increases alkaline phosphatase (ALP) activity and promotes the expression of genes encoding bone morphogenic protein-2, type I collagen, and osteocalcin, indicating its ability to induce proliferation and maturation of osteoblasts<sup>19–23</sup>. However, its application to titanium implants has shown varying results, as is also the case with the use of bisphosphonates in such implants<sup>24,25</sup>. In order to avoid potential complications from systemic application, several attempts have been made to administer alendronates locally and therefore to restrict ALN-induced osteoblastic activity to peri-implant bone regions<sup>26,27</sup>. A recent study suggesting the concurrent application of UV irradiation and ALN soaking to the titanium surfaces represents an example of such attempts<sup>28</sup>.

The long-term success of implant treatments requires not only the osseointegration of implant fixtures but also a rigid and tight seal around the implant abutments. Peri-implant soft tissues prevent subgingival biofilm formation through proper sealing and exhibit the potential to defend against bacterial penetration; these properties are important for implant maintenance and oral hygiene control<sup>7,29–31</sup>. Several studies have been carried out to improve the adhesion of soft tissue on implant abutment surfaces<sup>32–34</sup>. However, limited number of studies have examined the effects of UV treatment on the relationship between the machined titanium surface and soft tissues; one study showed that the proliferation of human gingival fibroblasts (HGFs) was significantly increased depending on the thickness of TiO<sub>2</sub> in TiO<sub>2</sub>-coated titanium surfaces when UV irradiation was performed<sup>35</sup>.

Considering that implant abutments are in contact with soft tissues and are composed of machined surfaces, it is necessary to investigate the effects of surface treatment methods on machined surfaces and demonstrate the responses of HGFs. Moreover, when aiming to apply either or both surface treatment methods to tissue-level implants that have both machined and rough surfaces, it is crucial to determine the effects of surface treatment methods on the fibroblast response. However, to our knowledge, there are no reports describing the effects of ALN immersion on HGFs cultured on machined titanium surfaces. Furthermore, as simultaneous application of UV irradiation and ALN immersion had been conducted in osteoblast-like cells in a previous study, it is reasonable to apply similar approaches to the HGFs.

Hence, we aimed to evaluate the effects of UV treatment and ALN immersion on the responses of osteoblast-like cells cultured on titanium discs with rough surface, and to assess the effects of these treatments on the responses of HGFs cultured on titanium discs with machined surface. The experiments were divided into the investigation of two types of surfaces to resemble clinical situations: titanium discs with rough surfaces were used to represent implant fixtures and those with machined surfaces were used to represent implant abutments. Osteoblast-like cells were used to evaluate hard tissue reactions on titanium surfaces at the implant fixture level, while HGFs were used to assess soft tissue reactions on titanium surfaces at the implant abutment level. The effects of simultaneous application of UV irradiation and ALN immersion on the responses of osteoblast-like cells and HGFs were also investigated.

## Materials and Methods

**Preparation of titanium specimens.** Titanium specimens were prepared in the shape of discs (10-mm diameter and 2-mm thickness) from commercially pure grade IV titanium (Dentium Co., Suwon, Korea). One half of the specimens were in the sandblasted, large grit, and acid-etched (SLA) state, and the other half was left untreated, i.e., in the machined (MA) state. The SLA specimens were sandblasted with aluminium oxide (Al<sub>2</sub>O<sub>3</sub>) and acid-etched with hydrochloric acid (HCl), and were then used to evaluate the responses of osteoblast-like cells. The MA specimens were ultrasonically cleaned in soap solution for 4 h, rinsed in distilled water, dried with oil-free air, and used to evaluate the reaction of HGFs. The SLA specimens were subdivided into four groups ( $n = 12$  for each group); the discs in the S group received no further surface treatment, those in the SUV group were treated with UV irradiation, those in the SAN group were immersed in ALN, and those in the SUVAN group received both surface treatments. The MA specimens were also subdivided into four groups ( $n = 12$  for each group) in a similar manner as the SLA specimens, replacing S with M in the group names. In total, 96 titanium discs were used in this study (Table 1). All specimens were sealed individually and sterilised by gamma irradiation.

**UV treatment of titanium surfaces.** For UV-treated groups (SUV, SUVAN, MUV, and MUVAN), the specimens were exposed to UV radiation for 15 min under ambient conditions using a UV-light-emitting device (TheraBeam SuperOsseo; Ushio Inc., Tokyo, Japan) 24 h before cell culture. The UV light was delivered as mixed spectrum through single UV lamp at wavelengths of 360 and 250 nm<sup>36</sup>.

**ALN immersion of titanium surfaces.** Specimens from the SAN, SUVAN, MAN, and MUVAN groups were immersed in a solution of 10<sup>-3</sup> M ALN (Cayman Chemical, Ann Arbor, MI, USA) for 24 h. For the SUVAN and MUVAN groups, in which both surface treatment methods were applied, UV photofunctionalisation procedures preceded ALN immersion.

Group	S	SUV	SAN	SUVAN	M	MUV	MAN	MUVAN
Basic surface	SLA surface				Machined surface			
UV	X	O	X	O	X	O	X	O
ALN	X	X	O	O	X	X	O	O
Cell line	MG-63 human osteoblast-like cells				Primary gingival fibroblasts (HGF)			

**Table 1.** Classification of the experimental design. S and M groups served as control groups for each cell line.

**Cell culture.** MG-63 human osteoblast-like cells (KCLB No. 21427) were purchased from the Korean Cell Line Bank (KCLB, Seoul, Korea), and primary gingival fibroblasts (PCS-201-018) were purchased from the American Type Culture Collection (ATCC, Manassas, VA, USA). The cells were seeded on 10-cm tissue culture dishes in standard cell culture medium consisting of Dulbecco's modified Eagle's medium (Invitrogen, Waltham, MA, USA) containing 10% foetal bovine serum (Invitrogen) and antibiotics (50 U/mL penicillin G and 50 µg/mL streptomycin; Invitrogen). Samples were incubated at 37°C in a 5% CO<sub>2</sub>/95% air atmosphere at 100% relative humidity. The cell culture medium was changed every 2–3 days. When the cells reached 85–90% confluence, they were treated with a trypsin-ethylenediaminetetraacetic acid solution (Invitrogen), resuspended in culture medium, and seeded in new dishes at a 1/5 dilution.

**Scanning electron microscopy (SEM).** MG-63 cells and HGFs were used for SLA and MA discs, respectively and seeded at  $1 \times 10^4$  cells/disc on the surface of each specimen in a 24-well plate. After incubation for 24 h, a specimen from each of the eight groups was prefixed with Karnovsky's fixative (2% glutaraldehyde-paraformaldehyde; Invitrogen) in 0.1 M phosphate buffer (PB, pH 7.4) for 6 h and washed twice for 30 min in 0.1 M PB. The specimens were postfixed with 1% osmium tetroxide dissolved in 0.1 M PB for 1.5 h, and washed with 0.1 M PB for 10 min. Specimens were then dehydrated in increasing concentrations of ethanol (50%, 60%, 70%, 80%, 90%, 95%, and 100%), infiltrated with isoamyl acetate, and subjected to critical point drying (Leica EM CPD300; Leica Mikrosysteme GmbH, Vienna, Austria). The specimens were coated with platinum (5 nm thickness) using an ion coater (Leica EM ACE600; Leica Mikrosysteme GmbH) and evaluated by field-emission SEM (Merin; Carl Zeiss, Jena, Germany). Representative images were captured at specific magnifications (500x, 2000x).

**Proliferation assay.** 2-(2-Methoxy-4-nitrophenyl)-3-(4-nitrophenyl)-5-(2,4-disulfophenyl)-2H-tetrazolium, monosodium salt (WST-8) assays were used to assess cell proliferation. First, six SLA or MA discs from each group were distributed in 24-well plates. The cells were trypsinised, resuspended in culture medium, and seeded in 24-well plates on SLA or MA discs at  $1 \times 10^4$  cells/disc. Cells were then cultured for 4 h at 37°C in an atmosphere containing 5% CO<sub>2</sub>. The proliferation of MG-63 cells and HGFs was measured using Cell Counting Kit-8 (CCK-8; Dojindo, Kumamoto, Japan) according to the manufacturer's instructions. The cell suspensions in each group were inoculated into 96-well plates, and 10 µL of the CCK-8 solution was added to each well of the plate, being careful to avoid the formation of bubbles. After incubating the plate for 1 h, the optical density (OD) of the water-soluble, yellow-coloured formazan, WST-8, formed by vital cells in each well was measured at 450 nm using an automated microplate reader (VersaMax Tunable microplate reader; Molecular Devices Co., Sunnyvale, CA, USA).

**ALP activity assay.** Differentiation of MG-63 cells was assessed by evaluating ALP expression using a QuantiChrom ALP Assay Kit (BioAssay Systems, Hayward, CA, USA). Five specimens from each of the four SLA groups (S, SUV, SAN, and SUVAN) were placed in 24-well plates;  $1 \times 10^4$  cells were seeded on each specimen and cultured for 3 days at 37°C in an atmosphere containing 5% CO<sub>2</sub>. Working solutions/reagents were prepared for each 96-well assay with 200 µL assay buffer, 5 µL magnesium acetate, and 2 µL *p*-nitrophenyl phosphate. Cells seeded on the discs were washed with phosphate-buffered saline (Invitrogen) and then lysed in 0.5 mL of 0.5% Triton X-100 for 20 min. Next, 5 µL of cell lysate mixed with 195 µL working solution was transferred to each well of the 96-well plate, and the ODs of each well were read at 405 nm at 0 and 4 min on a plate reader. ALP activities of the sample (IU/L = µmol/[L × min]) were calculated using the formula below:

$$\begin{aligned}
 &= \frac{(OD_{Sample\ t} - OD_{Sample\ 0}) \times 1000 \times Reaction\ Vol}{t \times \epsilon \times l \times Sample\ Vol} \\
 &= \frac{(OD_{Sample\ t} - OD_{Sample\ 0}) \times 1000 \times Reaction\ Vol}{(OD_{Calibrator} - OD_{H_2O}) \times Sample\ Vol \times t} \times 35.3
 \end{aligned}$$

**Real-time reverse transcription polymerase chain reaction (RT-PCR) analysis.** To evaluate the differentiation of HGFs, mRNA levels of integrin-β1, type I and III collagens, fibronectin, and laminin5 were analysed by RT-PCR. HGFs were cultured at  $1 \times 10^4$  cells/disc for 24 h on five discs from each of M, MUV, MAN, and MUVAN groups, and total RNA was isolated with a Hybrid-R kit (GeneAll Biotechnology Co., Ltd., Seoul, Korea). cDNA was synthesised using a Maxime RT Premix kit (iNtRON Biotechnology, Sungnam, Korea) according to the manufacturer's recommendations. Gene expression analysis was carried out using a SensiFAST SYBR Hi-ROX Kit (Bioline USA Inc., Taunton, MA, USA) on an ABI StepOnePlus Real-Time PCR machine (Applied Biosystems, Foster City, CA, USA). The specific amplification primers were from Integrated DNA Technologies (Coralville, IA, USA; Table 2).

	Forward primers (5' → 3')	Reverse primers (5' → 3')	Product length (bp)
Integrin-β1	TGTAAGGAGAAGGATGTTGACG	CAACCACACCAGCTACAATTG	142
Type I collagen	CCCCTGGAAAGAATGGAGATG	TCCAAACCACTGAAACCTCTG	148
Type III collagen	AAGTCAAGGAGAAAGTGGTCG	CTCGTTCTCCATTCTTACCAGG	125
Fibronectin	ACTGTACATGCTTCGGTCAG	AGTCTCTGAATCCTGGCATTG	74
Laminin5	CAAATGTGACCAGTGCAGC	CATCCCTCCATATCCACGAAC	144

**Table 2.** Lists of primer sequences used for RT-PCR analysis in this study.

**Statistical analysis.** The OD values measured by WST-8 assays and the results of ALP activity assays and RT-PCR were analysed by one-way analysis of variance. Bonferroni post-hoc tests were performed for pairwise comparisons of OD, ALP activity, and RT-PCR data. All statistical analyses were performed using IBM SPSS statistics software (version 23; SPSS Inc., Chicago, IL, USA) and the level of significance was set as  $\alpha = 0.05$ .

## Results

**Cellular attachment and morphology of MG-63 cells and HGFs on titanium surfaces.** SEM was used to qualitatively assess cellular attachment and cell morphology on titanium surfaces. MG-63 cells on SLA discs (groups S, SUV, SAN, and SUVAN) grew normally, regardless of surface treatment methods applied, and actively adhered to the titanium surfaces (Fig. 1a). At a higher magnification (2000x; Fig. 1b), extracellular vesicles were observed. For HGFs grown on MA discs (groups M, MUV, MAN, and MUVAN), the cells grew in a concentric dispersion, following the lines on the titanium surfaces (Fig. 2a). When observed at a higher magnification (2000x; Fig. 2b), typical features of cell adhesion, such as cytoplasmic prolongation and filopodia, were observed. In the middle portion of the discs, the cellular attachment pattern appeared similar among groups, whereas around the border of the discs, MAN and MUVAN groups showed fewer exosomes and microfilaments, and the cells were thinner.

**Proliferation of MG-63 cells and HGFs.** After 4 h of cell culture, the OD values of the SAN and SUVAN groups were significantly lower than those of the S and SUV groups ( $P < 0.05$ ; Fig. 3a). For HGFs, the MUV group showed a higher OD value than the M group, although the results were not statistically significant. Additionally, the MUVAN group showed the lowest value, which was significantly lower than that in the MUV group ( $P < 0.05$ ; Fig. 3b).

**Differentiation of MG-63 cells.** ALP activity in the S group did not differ from that in the SUV group. However, the SUVAN group showed significantly higher ALP activity than the S group ( $P < 0.05$ ). The ALP activity of the SUVAN group was significantly higher than that of the SAN group ( $P < 0.05$ ), but did not differ from that of the SUV group ( $P > 0.05$ ; Fig. 4).

**Differentiation of HGFs.** The mRNA levels of integrin-β1, type I and III collagen, fibronectin, and laminin5 in the MUV group were significantly higher than those in the M, MAN, and MUVAN groups ( $P < 0.05$ ; Fig. 5). However, there were no statistically significant differences between the mRNA levels of all the target genes in the M, MAN, and MUVAN groups ( $P > 0.05$ ; Fig. 5).

## Discussion

In order to improve the initial stability and achieve long-term success of implant treatments, numerous studies have been carried out to evaluate the biological responses on various kinds of implant surfaces at cellular levels<sup>37,38</sup>. As a result, it is generally accepted that rough surfaces are suitable for implant fixtures, whereas machined or turned surfaces are recommended for implant abutments<sup>39</sup>. However, various approaches to modify surfaces of the implants are still being developed to overcome a drawback resulting from the inherent properties of the titanium material itself<sup>40,41</sup>. The present study aimed to assess the potential utility of applying UV and/or ALN concurrently on both surfaces.

The SLA surface is manufactured by sandblasting with large grit particles, followed by acid-etching procedures with HCl/H<sub>2</sub>SO<sub>4</sub>, resulting in a rough surface<sup>42</sup>. All of the surface treatments applied to SLA surfaces showed favourable cell adhesion and maturation of extracellular matrix (ECM) in the present study, as shown by the SEM images, indicating that the surface treatments did not inhibit the growth and differentiation of MG-63 cells. The MG-63 cells in the SUVAN group exhibited significantly lower mitochondrial activity than those in the S group, as indicated by the cell proliferation assay<sup>43</sup>; however, they showed increased ALP activity relative to those in the S group. This can be explained by the proliferation/differentiation interrelationships during the progressive development of the osteoblast phenotype<sup>44,45</sup>. Osteoblasts undergo a sequential pattern of gene expression as differentiation progresses: (1) proliferation and ECM biosynthesis, (2) ECM development, maturation, and organisation, and (3) ECM mineralisation<sup>44</sup>. The ECM undergoes a series of changes in its configuration and structure during the immediate post-proliferative periods<sup>44</sup>. Further, as the mineralisation phase progresses, ALP activity shows early and progressively enhanced expression<sup>44,46</sup>. In the SAN group, the effects of ALN application alone on the response of MG-63 were unclear; in the SUV group, UV application alone did not elicit remarkable differences when compared with that in the S group. On the other hand, the concurrent application of UV treatment and ALN immersion facilitated the differentiation of MG-63 cells in the SUVAN group.

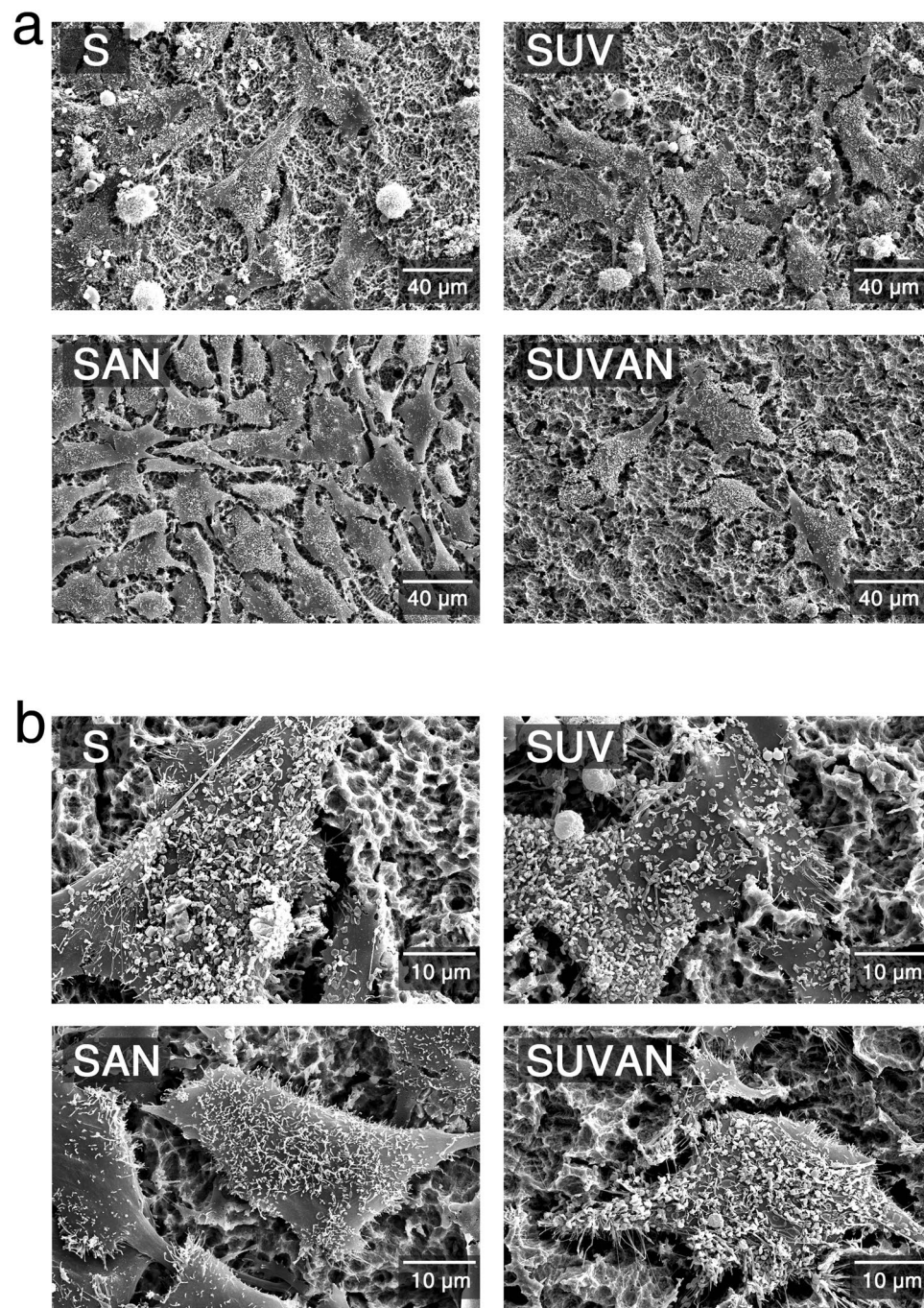


**Figure 1.** Representative SEM images of MG-63 cells cultured on titanium surfaces in the S, SUV, SAN, and SUVAN groups. (a) SEM images at 500x magnification, (b) SEM images at 2000x magnification.

The synergistic effects described above can be explained from a methodological standpoint related to the loading protocol of ALNs on titanium surfaces. When delivering biomolecules onto the implant surfaces, several methods, such as adsorption, covalent immobilisation, or release from coatings, are available<sup>47</sup>. As methods to facilitate the loading of ALNs, the use of pre-coated hydroxyapatite layers<sup>26</sup> or plasma treatment have been suggested<sup>27</sup>. Another strategy is to apply UV irradiation: it has been hypothesised that UV irradiation of titanium surface causes the removal of surface hydrocarbons owing to the photocatalytic activity of TiO<sub>2</sub>, and that the resulting exposed Ti<sup>4+</sup> sites attract ALN molecules. This is because ALNs are negatively charged at physiological pH<sup>48,49</sup>. This difference in charge enables ALNs to bind to the titanium surface more easily, and subsequently, facilitates the local apposition of ALNs through the hybridised mechanism of adsorption and release from coatings. The present study also demonstrated that the concurrent application of ALNs and UV treatment of SLA titanium surfaces resulted in an enhanced impact on osteoblast differentiation.

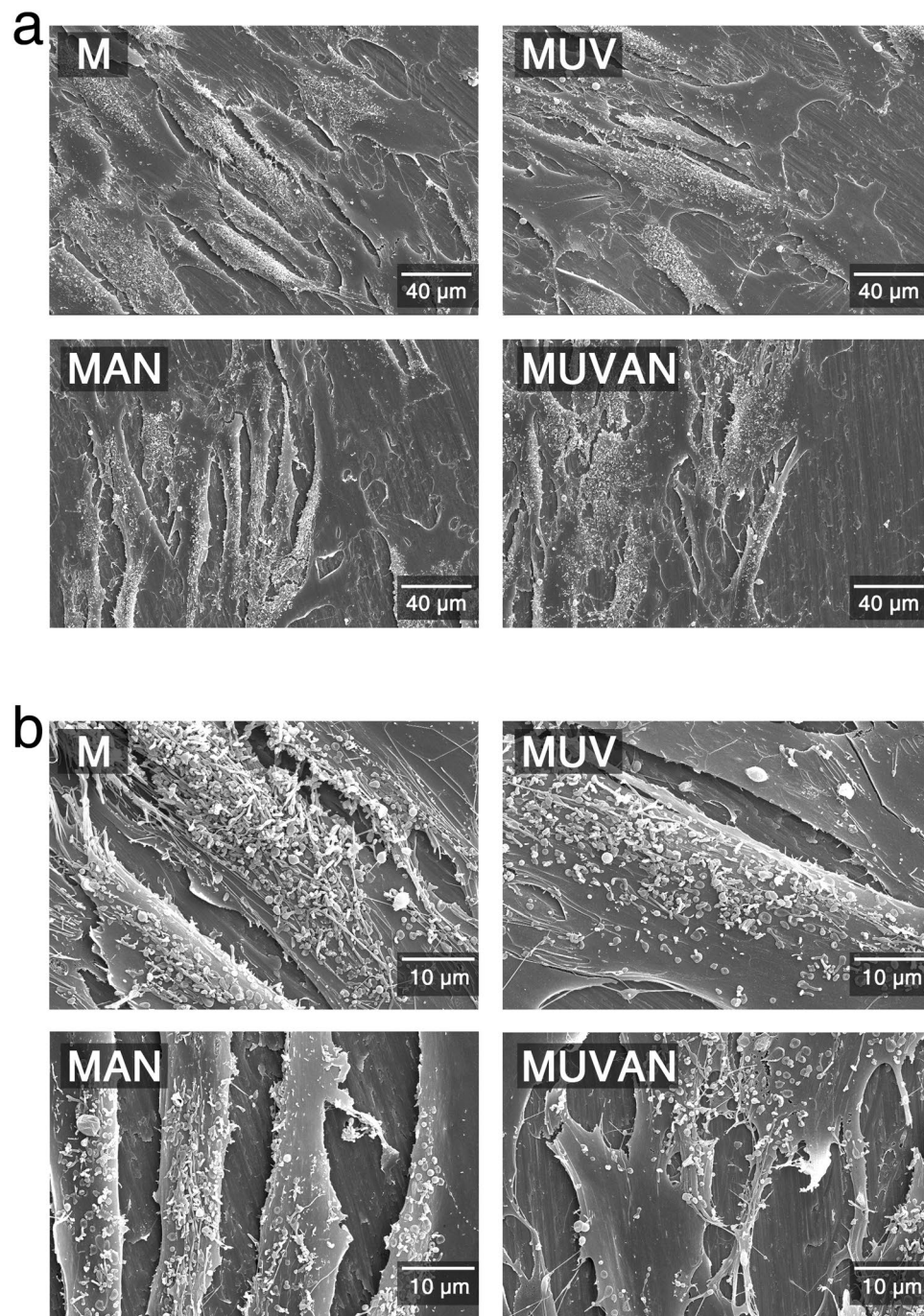


**Figure 2.** Representative SEM images of HGFs cultured on titanium surfaces in the M, MUV, MAN, and MUVAN groups. **(a)** SEM images at 500x magnification, **(b)** SEM images at 2000x magnification.

UV treatment of  $\text{TiO}_2$  surface causes the excitement of an electron from the valence band to the conduction band and creates a positive hole on the superficial layer<sup>50</sup>. This is followed by the transition process of electrons, causing catalysing chemical reactions. As a result, reactive oxygen species are produced at the surface of  $\text{TiO}_2$ , which enables removal of hydrocarbon through the reaction of such radicals<sup>51,52</sup>. In addition to this principle, direct UV irradiation itself also affects dissociation of hydrocarbons<sup>53</sup>. Through these processes, the titanium surface becomes more hydrophilic and acquires positive charge transforming from its original electrostatic state into a surface with higher bioactivity, and exhibits enhanced protein adsorption and cellular adhesion<sup>48</sup>. However, there were no remarkable differences in the response of MG-63 cells between the SUV and S groups in the present study. Further studies under different culture conditions are required for clarification.

The contamination of titanium surfaces is attributed to the accumulation of hydrocarbon on titanium surfaces over time<sup>11,53</sup>. From a physicochemical point of view, titanium surfaces are known to continuously absorb organic impurities, such as polycarbonate and hydrocarbons, through the atmosphere, water, and cleaning liquids<sup>54-56</sup>.

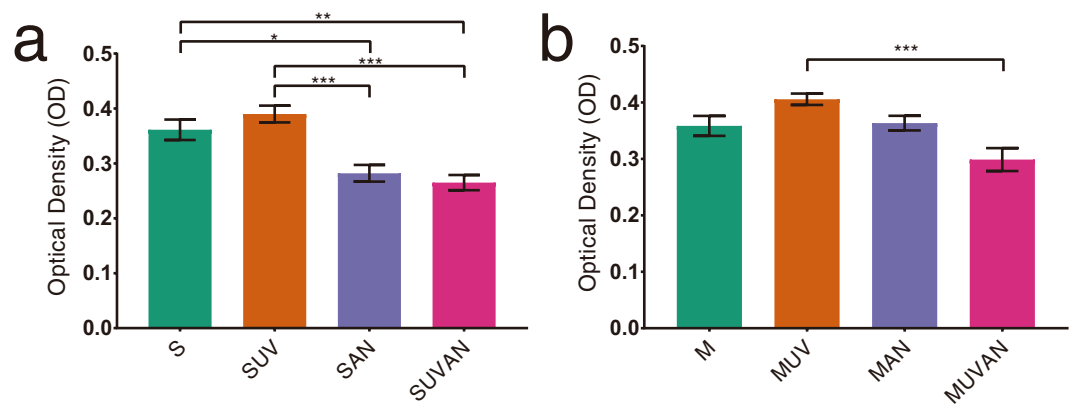


**Figure 3.** Effects of UV treatment and ALN immersion on cellular proliferation, as determined using WST-8 assays. Cellular proliferation was expressed as optical density (OD). (a) OD of MG-63 cells in the S, SUV, SAN, and SUVAN groups; (b) OD of HGFs in the M, MUV, MAN, and MUVAN groups. Data are expressed as means  $\pm$  S.E.M. ( $n = 6$ ). \* $P < 0.05$ , \*\* $P < 0.01$ , \*\*\* $P < 0.001$  for comparisons among groups. The asterisks indicate statistically significant differences between the groups.

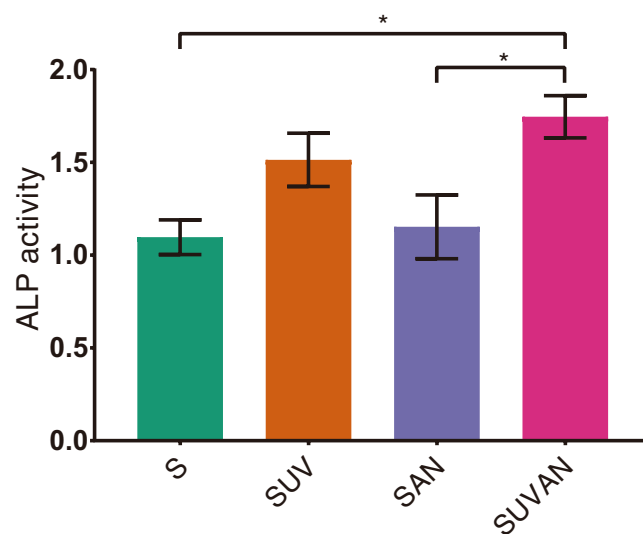


**Figure 4.** Effects of UV treatment and ALN immersion on ALP activity in MG-63 cells, as assessed by spectrophotometry after 3 days of culture, in the S, SUV, SAN, and SUVAN groups. Data are expressed as means  $\pm$  S.E.M. ( $n = 5$ ). \* $P < 0.05$  for comparisons among the groups. The asterisks indicate statistically significant differences between the groups.

More importantly, the rate and capacity to absorb proteins are critical factors in evaluating the biocompatibility of implant surfaces<sup>57</sup>, and are directly correlated with the amount of surface carbons<sup>11</sup>. This was demonstrated by a previous study in which aged titanium surfaces showed substantially reduced capacity to absorb proteins, and the early albumin adsorption rate was reduced after 4 weeks of storage compared with that of fresh surfaces<sup>10</sup>. Considerable reduction in fibronectin adsorption ability was also detected, although the degree of decomposition was lower than that of albumin<sup>10</sup>. Moreover, aged titanium surfaces were more hydrophobic than the fresh titanium surfaces<sup>53,58</sup>.

Fibroblasts use integrin receptors for their attachment; integrin- $\beta 1$  is an essential binding unit that enables the binding of fibroblasts to titanium surfaces<sup>59</sup>. Type I and III collagens are important constituents of ECM from healthy human gingiva<sup>60</sup>. Fibronectin and laminin5 are internal components of basement membrane and are proteins that contribute to cellular attachment<sup>61</sup>. Hence, we aimed to measure relative mRNA expression of the genes that encode these proteins. For the MUV group, mRNA expression of all the target genes exhibited significantly higher values compared with those of the other three groups, indicating that the photocatalytic activity of TiO<sub>2</sub> may also affect the attachment of fibroblasts on machined titanium surfaces<sup>35</sup>. Several attempts have been made to promote fibroblast attachment onto titanium surfaces<sup>62–64</sup>. However, to our knowledge, the present study is the first to use UV irradiation as a variable in evaluating its effect on fibroblasts cultured on machined titanium

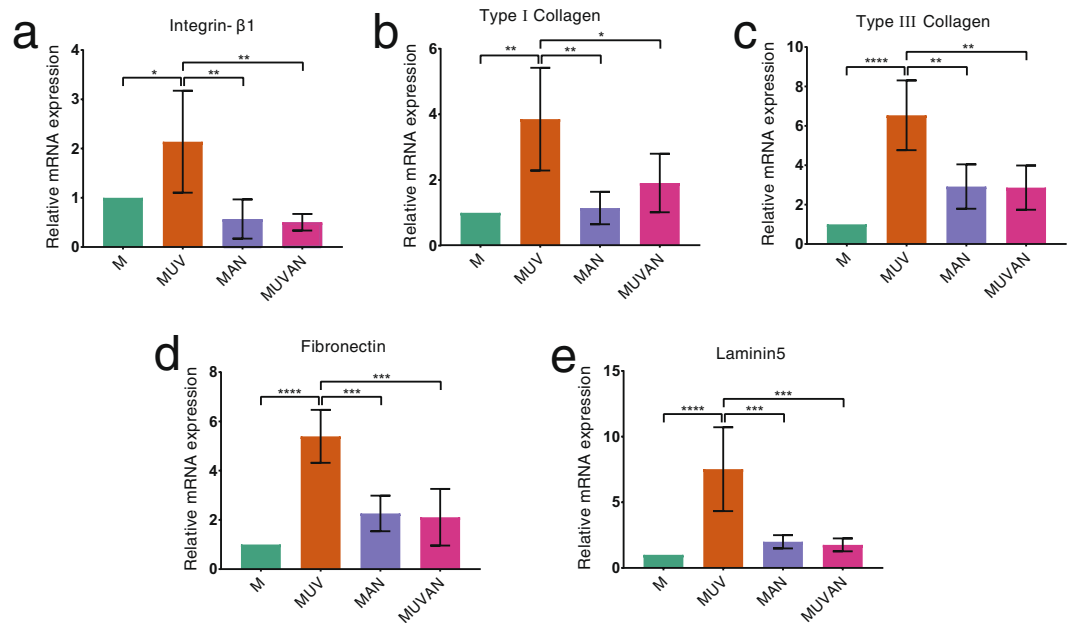


**Figure 5.** Effects of UV treatment and ALN immersion on cellular differentiation in HGFs in the M, MUV, MAN, and MUVAN groups. RT-PCR data indicate the relative mRNA expression of (a) integrin-β1, (b) type I collagen, (c) type III collagen, (d) fibronectin, and (e) laminin5 after 24 h of culture. Data are expressed as means ± S.E.M. ( $n = 5$ ). \* $P < 0.05$  for comparisons among the groups. The asterisks indicate statistically significant differences between the groups.

surfaces. Hence, as a technique to improve the long-term prognosis of implants, UV treatment of titanium abutment surfaces is worthy of further validation via *in vivo* studies.

In contrast, the role of ALN on fibroblasts requires further exploration; the SEM images exhibited atrophic and inactive morphology of HGFs in the ALN-treated groups (MAN and MUVAN). Previous studies also have shown that bisphosphonates had negative effects on oral mucosal cells<sup>26,65–67</sup>. However, the present study did not show significant differences in fibroblast attachment between the M and MUVAN groups. This result is in contrast with the results derived from SLA surfaces, in which concurrent application of UV treatment and ALN immersion showed synergetic effects. This may be attributed to the differences between machined and rough titanium surfaces; a previous study reported that the effects of soaking on machined titanium discs were less pronounced than those on rough titanium surfaces<sup>68</sup>. Hence, concurrent application of UV irradiation and ALN immersion on machined titanium surfaces appears to have little effect on fibroblasts.

There are several limitations to the present study. In the experiments using MG-63 cells, the discs of the SLA surface were used to represent implant fixtures. However, because the SLA surface itself has been shown to have a high success rate with regard to osseointegration of dental implants, differences from other surface treatment methods may not be conspicuous<sup>8,69</sup>. In addition, the disc-shaped material differed from the clinical environment. We used the commercially available MG-63 cell line in this study, which shows osteoblastic activities with high levels of ALP activity and osteocalcin production during differentiation<sup>70,71</sup>. Although MG-63 cells have characteristics comparable to human osteoblasts, further experiments using human osteoblasts are needed. Additionally, we applied ALN at a concentration of  $10^{-3}$  M. When MG-63 cells were exposed to  $10^{-8}$  to  $10^{-6}$  M ALN, the cellular activity of MG-63 cells was not altered. In contrast,  $10^{-3}$  to  $10^{-2}$  M ALN inhibited matrix metalloproteinases-2 activity in MG-63 cells<sup>72</sup>, and  $10^{-4}$  M ALN promoted the secretion of pro-inflammatory cytokines from human osteoblasts and reduced proliferation and differentiation<sup>73</sup>. These results were obtained by direct application of ALN solution. As we only immersed titanium discs in ALN, further studies are needed to identify the optimal ALN concentration for immersion.

It is necessary to distinguish between the effects of these surface treatments on the implant fixtures and implant abutments in order to apply these methods appropriately in clinical practice. For example, machined portion of the tissue-level implants, or implant abutments may not benefit from the concurrent application of UV irradiation and ALN immersion. Instead, it may be more reasonable to apply UV treatments on them. Moreover, the duration of UV treatment on the titanium surface may be an important issue with regard to implant abutments. In a recent study, the effects of UV treatment on the titanium surface were significantly reduced when the titanium was exposed to air for 28 days<sup>74</sup>. The procedures for dental prosthesis placement involve exposure of the abutments to air after they are fabricated; hence, it may be beneficial to apply UV treatment to abutments immediately before implant-abutment connection. Accordingly, a protocol to promote the early induction of mucosal sealing of the abutment by UV treatment may be designed. Further studies are needed to determine the duration for which these effects can be maintained and the effectiveness of this approach.

In summary, the present *in vitro* study highlights the feasibility of applying UV irradiation and ALN immersion as a strategy for the surface treatment of titanium discs. The results of this study extend our knowledge base



to further develop better technologies for the surface treatment of titanium implant fixtures and abutments. The study showed a significant improvement in osteoblastic activity by simultaneous application of UV treatment and ALN immersion to titanium discs with rough surfaces; however, the individual application of each method did not yield significant enhancement. With regard to titanium discs with machined surfaces, concurrent application of UV irradiation and ALN immersion did not increase fibroblast attachment. However, UV treatment of machined titanium surfaces was found to be effective for enhancing fibroblast attachment. Further *in vivo* studies are necessary for detailed evaluation of the effects of these surface treatment methods for titanium implants and abutments in animal models.

## Data Availability

The authors declare that all data supporting the findings of this study are available within the article or from the corresponding author upon reasonable request.

## References

- Brunette, D. M., Tengvall, P., Textor, M. & Thomsen, P. *Titanium in medicine: material science, surface science, engineering, biological responses and medical applications* (Springer Science & Business Media, 2012).
- Parr, G. R., Gardner, L. K. & Toth, R. W. Titanium: the mystery metal of implant dentistry. *Dental materials aspects. J Prosthet Dent* **54**, 410–414 (1985).
- Steinemann, S. G. Titanium—the material of choice? *Periodontol* **2000** **17**, 7–21 (1998).
- Walivaara, B., Aronsson, B. O., Rodahl, M., Lausmaa, J. & Tengvall, P. Titanium with different oxides: *in vitro* studies of protein adsorption and contact activation. *Biomaterials* **15**, 827–834 (1994).
- Ellingsen, J. E. A study on the mechanism of protein adsorption to TiO<sub>2</sub>. *Biomaterials* **12**, 593–596 (1991).
- Albrektsson, T., Bränemark, P.-I. & Zarb, G. A. *Tissue-integrated Prostheses: Osseointegration in Clinical Dentistry* (Quintessence, 1985).
- Elter, C. *et al.* Supra- and subgingival biofilm formation on implant abutments with different surface characteristics. *Int J Oral Maxillofac Implants* **23**, 327–334 (2008).
- Cochran, D. L., Schenk, R. K., Lussi, A., Higginbottom, F. L. & Buser, D. Bone response to unloaded and loaded titanium implants with a sandblasted and acid-etched surface: a histometric study in the canine mandible. *J Biomed Mater Res* **40**, 1–11 (1998).
- De Bruyn, H. *et al.* Implant surface roughness and patient factors on long-term peri-implant bone loss. *Periodontol* **2000** **73**, 218–227, <https://doi.org/10.1111/prd.12177> (2017).
- Hori, N. *et al.* Ultraviolet light treatment for the restoration of age-related degradation of titanium bioactivity. *Int J Oral Maxillofac Implants* **25**, 49–62 (2010).
- Att, W. *et al.* Time-dependent degradation of titanium osteoconductivity: an implication of biological aging of implant materials. *Biomaterials* **30**, 5352–5363, <https://doi.org/10.1016/j.biomaterials.2009.06.040> (2009).
- Wang, R. *et al.* Light-induced amphiphilic surfaces. *Nature* **388**, 431 (1997).
- Ogawa, T. Ultraviolet photofunctionalization of titanium implants. *Int J Oral Maxillofac Implants* **29**, e95–102, <https://doi.org/10.11607/jomi.te47> (2014).
- Russell, R. G. Bisphosphonates: from bench to bedside. *Ann N Y Acad Sci* **1068**, 367–401, <https://doi.org/10.1196/annals.1346.041> (2006).
- von Knoch, F. *et al.* Effects of bisphosphonates on proliferation and osteoblast differentiation of human bone marrow stromal cells. *Biomaterials* **26**, 6941–6949, <https://doi.org/10.1016/j.biomaterials.2005.04.059> (2005).
- Fromigie, O. & Body, J. J. Bisphosphonates influence the proliferation and the maturation of normal human osteoblasts. *J Endocrinol Invest* **25**, 539–546, <https://doi.org/10.1007/bf03345497> (2002).
- Im, G. I., Qureshi, S. A., Kenney, J., Rubash, H. E. & Shanbhag, A. S. Osteoblast proliferation and maturation by bisphosphonates. *Biomaterials* **25**, 4105–4115, <https://doi.org/10.1016/j.biomaterials.2003.11.024> (2004).
- Reinholz, G. G. *et al.* Bisphosphonates directly regulate cell proliferation, differentiation, and gene expression in human osteoblasts. *Cancer Res* **60**, 6001–6007 (2000).
- Xiong, Y., Yang, H. J., Feng, J., Shi, Z. L. & Wu, L. D. Effects of alendronate on the proliferation and osteogenic differentiation of MG-63 cells. *J Int Med Res* **37**, 407–416, <https://doi.org/10.1177/147323000903700216> (2009).
- Drake, M. T., Clarke, B. L. & Khosla, S. Bisphosphonates: mechanism of action and role in clinical practice. *Mayo Clin Proc* **83**, 1032–1045, <https://doi.org/10.4065/83.9.1032> (2008).
- Fleisher, K. E. *et al.* Predicting risk for bisphosphonate-related osteonecrosis of the jaws: CTX versus radiographic markers. *Oral Surg Oral Med Oral Pathol Oral Radiol Endod* **110**, 509–516, <https://doi.org/10.1016/j.tripleo.2010.04.023> (2010).
- Russell, R. G. Bisphosphonates: the first 40 years. *Bone* **49**, 2–19, <https://doi.org/10.1016/j.bone.2011.04.022> (2011).
- Kuhl, S., Walter, C., Acham, S., Pfeffer, R. & Lambrecht, J. T. Bisphosphonate-related osteonecrosis of the jaws—a review. *Oral Oncol* **48**, 938–947, <https://doi.org/10.1016/j.oraloncology.2012.03.028> (2012).
- Back, D. A. *et al.* Effect of local zoledronate on implant osseointegration in a rat model. *BMC Musculoskelet Disord* **13**, 42, <https://doi.org/10.1186/1471-2474-13-42> (2012).
- Chacon, G. E., Stine, E. A., Larsen, P. E., Beck, F. M. & McGlumphy, E. A. Effect of alendronate on endosseous implant integration: an *in vivo* study in rabbits. *J Oral Maxillofac Surg* **64**, 1005–1009, <https://doi.org/10.1016/j.joms.2006.01.007> (2006).
- Hu, X., Neoh, K. G., Shi, Z., Kang, E. T. & Wang, W. An *in vitro* assessment of fibroblast and osteoblast response to alendronate-modified titanium and the potential for decreasing fibrous encapsulation. *Tissue Eng Part A* **19**, 1919–1930, <https://doi.org/10.1089/ten.TEA.2012.0218> (2013).
- Zheng, D., Neoh, K. G. & Kang, E. T. Immobilization of alendronate on titanium via its different functional groups and the subsequent effects on cell functions. *J Colloid Interface Sci* **487**, 1–11, <https://doi.org/10.1016/j.jcis.2016.10.014> (2017).
- Kim, H. S. *et al.* The effect of alendronate soaking and ultraviolet treatment on bone-implant interface. *Clin Oral Implants Res* **28**, 1164–1172, <https://doi.org/10.1111/clr.12933> (2017).
- Berglundh, T., Lindhe, J., Marinello, C., Ericsson, I. & Liljenberg, B. Soft tissue reaction to de novo plaque formation on implants and teeth. An experimental study in the dog. *Clin Oral Implants Res* **3**, 1–8 (1992).
- Rasperini, G., Maglione, M., Cocconcelli, P. & Simion, M. *In vivo* early plaque formation on pure titanium and ceramic abutments: a comparative microbiological and SEM analysis. *Clin Oral Implants Res* **9**, 357–364 (1998).
- Bollen, C. M., Lambrechts, P. & Quirynen, M. Comparison of surface roughness of oral hard materials to the threshold surface roughness for bacterial plaque retention: a review of the literature. *Dent Mater* **13**, 258–269 (1997).
- Guida, L. *et al.* Human gingival fibroblast functions are stimulated by oxidized nano-structured titanium surfaces. *J Dent* **41**, 900–907, <https://doi.org/10.1016/j.jdent.2013.07.009> (2013).
- Lee, D. W. *et al.* Effect of laser-dimpled titanium surfaces on attachment of epithelial-like cells and fibroblasts. *J Adv Prosthodont* **7**, 138–145, <https://doi.org/10.4047/jap.2015.7.2.138> (2015).

34. Khadra, M., Kasem, N., Lyngstadaas, S. P., Haanaes, H. R. & Mustafa, K. Laser therapy accelerates initial attachment and subsequent behaviour of human oral fibroblasts cultured on titanium implant material. A scanning electron microscope and histomorphometric analysis. *Clin Oral Implants Res* **16**, 168–175, <https://doi.org/10.1111/j.1600-0501.2004.01092.x> (2005).
35. Hoshi, N., Negishi, H., Okada, S., Nonami, T. & Kimoto, K. Response of human fibroblasts to implant surface coated with titanium dioxide photocatalytic films. *J Prosthodont Res* **54**, 185–191, <https://doi.org/10.1016/j.jpor.2010.04.005> (2010).
36. Tuna, T., Wein, M., Swain, M., Fischer, J. & Att, W. Influence of ultraviolet photofunctionalization on the surface characteristics of zirconia-based dental implant materials. *Dent Mater* **31**, e14–24, <https://doi.org/10.1016/j.dental.2014.10.008> (2015).
37. Goldman, M., Juodzbaly, G. & Vilkinis, V. Titanium surfaces with nanostructures influence on osteoblasts proliferation: a systematic review. *J Oral Maxillofac Res* **5**, e1, <https://doi.org/10.5037/jomr.2014.5301> (2014).
38. Att, W., Yamada, M. & Ogawa, T. Effect of titanium surface characteristics on the behavior and function of oral fibroblasts. *Int J Oral Maxillofac Implants* **24**, 419–431 (2009).
39. Rompen, E., Domken, O., Degidi, M., Pontes, A. E. & Piattelli, A. The effect of material characteristics, of surface topography and of implant components and connections on soft tissue integration: a literature review. *Clin Oral Implants Res* **17**(Suppl 2), 55–67, <https://doi.org/10.1111/j.1600-0501.2006.01367.x> (2006).
40. Spriano, S., Yamaguchi, S., Bairo, F. & Ferraris, S. A critical review of multifunctional titanium surfaces: New frontiers for improving osseointegration and host response, avoiding bacteria contamination. *Acta Biomater* **79**, 1–22, <https://doi.org/10.1016/j.actbio.2018.08.013> (2018).
41. Civantos, A. *et al.* Titanium coatings and surface modifications: toward clinically useful bioactive implants. *ACS Biomaterials Science & Engineering* **3**, 1245–1261 (2017).
42. Smeets, R. *et al.* Impact of Dental Implant Surface Modifications on Osseointegration. *Biomed Res Int* **2016**, 6285620, <https://doi.org/10.1155/2016/6285620> (2016).
43. Berridge, M. V., Herst, P. M. & Tan, A. S. Tetrazolium dyes as tools in cell biology: new insights into their cellular reduction. *Biotechnol Annu Rev* **11**, 127–152, [https://doi.org/10.1016/s1387-2656\(05\)11004-7](https://doi.org/10.1016/s1387-2656(05)11004-7) (2005).
44. Stein, G. S. & Lian, J. B. Molecular mechanisms mediating proliferation/differentiation interrelationships during progressive development of the osteoblast phenotype. *Endocr Rev* **14**, 424–442, <https://doi.org/10.1210/edrv-14-4-424> (1993).
45. Bidwell, J. P. *et al.* Nuclear matrix proteins distinguish normal diploid osteoblasts from osteosarcoma cells. *Cancer Res* **54**, 28–32 (1994).
46. Vukicevic, S., Luyten, F. P., Kleinman, H. K. & Reddi, A. H. Differentiation of canalicular cell processes in bone cells by basement membrane matrix components: regulation by discrete domains of laminin. *Cell* **63**, 437–445 (1990).
47. Puleo, D. A. & Nanci, A. Understanding and controlling the bone-implant interface. *Biomaterials* **20**, 2311–2321 (1999).
48. Iwasa, F. *et al.* Enhancement of osteoblast adhesion to UV-photofunctionalized titanium via an electrostatic mechanism. *Biomaterials* **31**, 2717–2727, <https://doi.org/10.1016/j.biomaterials.2009.12.024> (2010).
49. Epstein, H. *et al.* Nanosuspensions of alendronate with gallium or gadolinium attenuate neointimal hyperplasia in rats. *J Control Release* **117**, 322–332, <https://doi.org/10.1016/j.jconrel.2006.10.030> (2007).
50. Rapuano, B. E., Lee, J. J. & MacDonald, D. E. Titanium alloy surface oxide modulates the conformation of adsorbed fibronectin to enhance its binding to alpha(5)beta(1) integrins in osteoblasts. *Eur J Oral Sci* **120**, 185–194, <https://doi.org/10.1111/j.1600-0722.2012.954.x> (2012).
51. Harper, J., Christensen, P., Egerton, T., Curtis, T. & Gunlazuardi, J. Effect of catalyst type on the kinetics of the photoelectrochemical disinfection of water inoculated with *E. coli*. *Journal of Applied Electrochemistry* **31**, 623–628 (2001).
52. Foster, H. A., Ditta, I. B., Varghese, S. & Steele, A. Photocatalytic disinfection using titanium dioxide: spectrum and mechanism of antimicrobial activity. *Appl Microbiol Biotechnol* **90**, 1847–1868, <https://doi.org/10.1007/s00253-011-3213-7> (2011).
53. Att, W. *et al.* The effect of UV-photofunctionalization on the time-related bioactivity of titanium and chromium-cobalt alloys. *Biomaterials* **30**, 4268–4276, <https://doi.org/10.1016/j.biomaterials.2009.04.048> (2009).
54. Kasemo, B. & Lausmaa, J. Biomaterial and implant surfaces: on the role of cleanliness, contamination, and preparation procedures. *J Biomed Mater Res* **22**, 145–158 (1988).
55. Kilpadi, D. V. *et al.* Cleaning and heat-treatment effects on unalloyed titanium implant surfaces. *Int J Oral Maxillofac Implants* **15**, 219–230 (2000).
56. Serro, A. P. & Saramago, B. Influence of sterilization on the mineralization of titanium implants induced by incubation in various biological model fluids. *Biomaterials* **24**, 4749–4760 (2003).
57. Woo, K. M., Seo, J., Zhang, R. & Ma, P. X. Suppression of apoptosis by enhanced protein adsorption on polymer/hydroxyapatite composite scaffolds. *Biomaterials* **28**, 2622–2630, <https://doi.org/10.1016/j.biomaterials.2007.02.004> (2007).
58. Att, W. & Ogawa, T. Biological aging of implant surfaces and their restoration with ultraviolet light treatment: a novel understanding of osseointegration. *Int J Oral Maxillofac Implants* **27**, 753–761 (2012).
59. Kramer, P. R., Janik Keith, A., Cai, Z., Ma, S. & Watanabe, I. Integrin mediated attachment of periodontal ligament to titanium surfaces. *Dent Mater* **25**, 877–883, <https://doi.org/10.1016/j.dental.2009.01.095> (2009).
60. Narayanan, A. S. & Page, R. C. Connective tissues of the periodontium: a summary of current work. *Coll Relat Res* **3**, 33–64 (1983).
61. Martinez-Hernandez, A. & Amenta, P. S. The basement membrane in pathology. *Lab Invest* **48**, 656–677 (1983).
62. Lee, J. H., Kim, Y. H., Choi, E. H., Kim, K. M. & Kim, K. N. Air atmospheric-pressure plasma-jet treatment enhances the attachment of human gingival fibroblasts for early peri-implant soft tissue seals on titanium dental implant abutments. *Acta Odontol Scand* **73**, 67–75, <https://doi.org/10.3109/00016357.2014.954265> (2015).
63. Al Mustafa, M., Agis, H., Muller, H. D., Watzek, G. & Gruber, R. *In vitro* adhesion of fibroblastic cells to titanium alloy discs treated with sodium hydroxide. *Clin Oral Implants Res* **26**, 15–19, <https://doi.org/10.1111/clr.12294> (2015).
64. Middleton, C. A., Pendegrass, C. J., Gordon, D., Jacob, J. & Blunn, G. W. Fibronectin silanized titanium alloy: a bioinductive and durable coating to enhance fibroblast attachment *in vitro*. *J Biomed Mater Res A* **83**, 1032–1038, <https://doi.org/10.1002/jbm.a.31382> (2007).
65. Ravosa, M. J., Ning, J., Liu, Y. & Stack, M. S. Bisphosphonate effects on the behaviour of oral epithelial cells and oral fibroblasts. *Arch Oral Biol* **56**, 491–498, <https://doi.org/10.1016/j.archoralbio.2010.11.003> (2011).
66. Walter, C. *et al.* Influence of bisphosphonates on endothelial cells, fibroblasts, and osteogenic cells. *Clin Oral Investig* **14**, 35–41, <https://doi.org/10.1007/s00784-009-0266-4> (2010).
67. Basso, F. G. *et al.* Cytotoxic effects of zoledronic acid on human epithelial cells and gingival fibroblasts. *Braz Dent J* **24**, 551–558, <https://doi.org/10.1590/0103-6440201302229> (2013).
68. Vanzillotta, P. S., Sader, M. S., Bastos, I. N. & Soares Gde, A. Improvement of *in vitro* titanium bioactivity by three different surface treatments. *Dent Mater* **22**, 275–282, <https://doi.org/10.1016/j.dental.2005.03.012> (2006).
69. Li, D. H., Liu, B. L., Zou, J. C. & Xu, K. W. Improvement of osseointegration of titanium dental implants by a modified sandblasting surface treatment: an *in vivo* interfacial biomechanics study. *Implant Dent* **8**, 289–294 (1999).
70. Schwartz, Z. *et al.* Local factor production by MG63 osteoblast-like cells in response to surface roughness and 1,25-(OH)<sub>2</sub>D<sub>3</sub> is mediated via protein kinase C- and protein kinase A-dependent pathways. *Biomaterials* **22**, 731–741 (2001).
71. Kim, H. J. *et al.* Varying Ti-6Al-4V surface roughness induces different early morphologic and molecular responses in MG63 osteoblast-like cells. *J Biomed Mater Res A* **74**, 366–373, <https://doi.org/10.1002/jbm.a.30327> (2005).
72. Sun, J., Song, F., Zhang, W., Sexton, B. E. & Windsor, L. J. Effects of alendronate on human osteoblast-like MG63 cells and matrix metalloproteinases. *Arch Oral Biol* **57**, 728–736, <https://doi.org/10.1016/j.archoralbio.2011.12.007> (2012).

73. Kruger, T. B., Herlofson, B. B., Landin, M. A. & Reseland, J. E. Alendronate alters osteoblast activities. *Acta Odontol Scand* **74**, 550–557, <https://doi.org/10.1080/00016357.2016.1217041> (2016).
74. Choi, S. H. *et al.* Overcoming the biological aging of titanium using a wet storage method after ultraviolet treatment. *Sci Rep* **7**, 3833, <https://doi.org/10.1038/s41598-017-04192-9> (2017).

### Acknowledgements

This research was supported by the Basic Science Research Program through the National Research Foundation of Korea (NRF) funded by the Ministry of Education (Grant No. NRF-2017R1D1A1B03034368).

### Author Contributions

C.J., K.C.O. and H.S.M. conceived the experiments. C.J., K.C.O. and K.H.P. conducted all the experiments. C.J. and K.C.O. interpreted and analysed the results. C.J. and K.C.O. conceived and wrote the manuscript. H.S.M. assisted writing and revising the manuscript. All authors reviewed and approved the final manuscript.

### Additional Information

**Competing Interests:** The authors declare no competing interests.

**Publisher's note:** Springer Nature remains neutral with regard to jurisdictional claims in published maps and institutional affiliations.



**Open Access** This article is licensed under a Creative Commons Attribution 4.0 International License, which permits use, sharing, adaptation, distribution and reproduction in any medium or format, as long as you give appropriate credit to the original author(s) and the source, provide a link to the Creative Commons license, and indicate if changes were made. The images or other third party material in this article are included in the article's Creative Commons license, unless indicated otherwise in a credit line to the material. If material is not included in the article's Creative Commons license and your intended use is not permitted by statutory regulation or exceeds the permitted use, you will need to obtain permission directly from the copyright holder. To view a copy of this license, visit <http://creativecommons.org/licenses/by/4.0/>.

© The Author(s) 2019